IN-85
53517
25 P.

DOE/NASA/50112-68
NASA TM-88898

Effect of Water on Hydrogen Permeability

David Hulligan
Sverdrup Technology

and

William A. Tomazic
National Aeronautics and Space Administration
Lewis Research Center

January 1987

Prepared for
U.S. DEPARTMENT OF ENERGY
Conservation and Renewable Energy
Office of Vehicle and Engine R&D

DISCLAIMER

Printed in the United States of America

Available from
National Technical Information Service
U.S. Department of Commerce
5285 Port Royal Road
Springfield, VA 22161

NTIS price codes[1]
Printed copy:
Microfiche copy: A02

[1]Codes are used for pricing all publications. The code is determined by the number of pages in the publication. Information pertaining to the pricing codes can be found in the current issues of the following publications, which are generally available in most libraries: *Energy Research Abstracts (ERA); Government Reports Announcements* and Index (*GRA* and I); *Scientific and Technical Abstract Reports (STAR)*: and publication, NTIS-PR-360 available from NTIS at the above address.

DOE/NASA/50112-68
NASA TM-88898

Effect of Water on Hydrogen Permeability

David Hulligan
Sverdrup Technology
Middleburg Heights, Ohio

and

William A. Tomazic
National Aeronautics and Space Administration
Lewis Research Center
Cleveland, Ohio 44135

January 1987

Prepared for
U.S. DEPARTMENT OF ENERGY
Conservation and Renewable Energy
Office of Vehicle and Engine R&D
Washington, D.C. 20545
Under Interagency Agreement DE-AI01-85CE50112

EFFECT OF WATER ON HYDROGEN PERMEABILITY

David Hulligan
Sverdrup Technology, Inc.
Lewis Research Center
Cleveland, Ohio 44135

and

William A. Tomazic
National Aeronautics and Space Administration
Lewis Research Center
Cleveland, Ohio 44135

SUMMARY

Doping of hydrogen with CO and CO_2 was developed to reduce hydrogen permeation in Stirling engines by forming a low permeability oxide coating on the inner surface of the heater head tubes. Although doping worked well, under certain circumstances the protective oxide could be chemically reduced by the hydrogen in the engine. Some oxygen is required in the hydrogen to prevent reduction. Eventually, all the oxygen in the hydrogen gas - whatever its source - shows up as water. This is the result of hydrogen reducing the CO, CO_2, or the protective inner surface oxides. This water can condense in the engine system under the right conditions. If the concentration of water vapor is reduced to a low enough level, the hydrogen can chemically reduce the oxide coating, resulting in an increase in permeability. This work was done to define the minimum water content required to avoid this reduction in the oxide coating. The results of this testing show that a minimum of approximately 750 ppm water is required to prevent an increase in permeability of CG-27, a high temperature metal alloy selected for Stirling engine heater tubes.

INTRODUCTION

Work has been done on high temperature alloys by NASA Lewis Research Center and its contractors as part of the U.S. Department of Energy Stirling engine development program. One aspect of this work has been to investigate the phenomenon of hydrogen permeability and to develop techniques for reducing it to an acceptable level for Stirling engine operation.

Hydrogen permeation in a Stirling engine occurs in the heater head which may range in temperature from 700 to 900 °C. Hydrogen permeation is the phenomenon of the hydrogen working fluid diffusing through the heater head material. This loss of hydrogen by permeation through the heater head is only one of the major leak paths, the other being leakage at static and dynamic seals. All of these must be minimized if the Stirling engine is to contain its working fluid. Failure to contain the hydrogen will mean that the engine will suffer from loss of power and will need to be recharged frequently.

A method called doping developed at the NASA Lewis can reduce permeability by an order of magnitude or more (ref. 1). This method consists of adding oxygen bearing gases to the hydrogen which results in the formation of an impermeable oxide layer on the inside of the heater head tubes. During later engine testing it was noticed that water had condensed in the area of the

engine cooler (ref. 2). This condensation showed that the Stirling engine was capable of removing oxygen from its working fluid in the form of water. This removal of oxygen implies the possibility of reducing the inner surface oxide and thus removing it or increasing its porosity, thereby increasing permeation of hydrogen through the heater head tubes.

The purpose of these experiments was to determine the minimum concentration of oxygen that is required to maintain the oxide coverage needed for stable low permeability. Test modules that had been previously oxidized using 1 percent CO_2 (by volume) doped H_2 to bring permeability down to a minimum value, were placed in an oil fired furnace. These modules were then filled with hydrogen having oxygen contents between 0 and 2,000 ppm. They were typically operated for 20 5-hr cycles. The modules were vented, evacuated, and refilled between each cycle. Permeability was calculated from the pressure decline that was observed for each module. The final results are shown in terms of permeability as a function of water content.

EQUIPMENT AND PROCEDURES

Materials

The material used in this testing was CG-27. This material is an iron-nickel based alloy and was selected as a Stirling engine heater head material because of its low strategic material content, high temperature creep strength (ref. 3) and low permeability with doped hydrogen (ref. 4). The nominal composition is 38 percent nickel, 13 percent chrome, 5.75 percent molybdenum, 1.6 percent aluminum, 2.5 percent titanium, 0.7 percent columbium, 0.05 percent carbon, 0.01 percent boron, and the balance iron.

The material was tested in the form of seamless tubing with an outside diameter of 4.5 mm and a wall thickness of 0.8 mm. The tubing was heat treated in a vacuum furnace prior to testing. This heat treatment resulted in the formation of a tough, adherent oxide on the surface of the material. The tubing still required additional conditioning in the rig with 1 percent CO_2 (by volume) doped hydrogen to achieve the desired low permeability. The temperatures and times at temperature are as follows:

1. 1500 °C, held for 10 min then furnace cooled to
2. 790 °C, held for 16 hr then furnace cooled to
3. 650 °C, held for 24 hr then
4. furnace cooled.

Simulator Rig

Figure 1 shows a schematic of the simulator rig that was used for this test program. This rig was used in previous permeability and endurance tests of candidate Stirling engine heater head materials (refs. 1 and 3 to 6). The test rig is basically a temperature-controlled oil-fired furnace with provisions for inserting up to 12 test modules. The hot combustion gases pass over the tube sets causing the formation of an oxide on the outside surface of the tubing material. The presence of this oxide results in a lower calculated permeability for the material (ref. 6). The outside oxide, without the inside oxide, is insufficient to reduce permeability to a low enough level for use in

an automotive Stirling engine (refs. 1 and 6). A test module consists of four u-shaped hairpin tubes, each with a half length of 30.5 cm, a stainless steel strain gage pressure transducer, two valves, and a copper manifold block. The hairpins and valves were attached to the manifold block with compression fittings. The pressure transducer was mounted on a water cooled block which was also attached with compression fittings. When inserted into the rig the manifold block was situated on water cooled copper plates with the temperature regulated to 82 °C. All test modules were bubble tight leak checked prior to insertion into the rig. Additional leak tests were periodically performed during the course of the test program. These periodic leak checks were typically done by monitoring the overnight leakage with high pressure gas while the modules were still in the rig. Any module that was found to be leaking was then serviced.

Procedures

All modules were initially oxidized by operating for 20 cycles of 5 hr each with 1 percent CO_2 (by volume) doped hydrogen so that they would be at a stable low permeability. Figure 2 shows how the rate of pressure decline is reduced as the inner oxide is built up.

A test with a specific gas typically consisted of twenty 5-hr cycles at a nominal temperature of 760 °C. Tests were run at nominal pressures of 3.4, 6.2, and 13.1 MPa. A specific purge and fill procedure was used prior to each test. This procedure consisted of inerting the contents of each module with three fills and evacuations with argon, followed by two fills and evacuations with low pressure hydrogen. Following the low pressure argon and hydrogen purges the modules were filled with the doped hydrogen being tested. Compositions of the doped hydrogen are given in table I. After filling with high pressure hydrogen, the heating cycle was started. The initial pressure measurement for permeation calculations was taken 24 min after the successful start, and the final pressure 5 hr after the start. Transducer drift was measured at the end of the run and was taken into account when calculating permeability. Each module was also evacuated at the end of each low level dopant run after it had cooled down to between 50 and 80 °C. Permeability was calculated from the rate of pressure decay at constant temperature using the technique described in reference 1.

An error analysis was performed to determine the accuracy of the calculated permeability. Any error in the measurement of the inital pressure, the final pressure, or the pressure change would result in some error in the calculated permeability. In general, this error band was found to be about $\pm 0.25 \times 10^{-6}$ $cm^2/sec\ MPa^{0.5}$. The size of the error band does vary with pressure level, however this value represents the average size of the error band.

BACKGROUND ANALYSIS

Hydrogen permeability in a Stirling engine is the phenomenon of the hydrogen diffusing through the engine heater head. Early testing showed permeabilities of 4 to 20×10^{-6} $cm^2/sec\ MPa^{0.5}$ when test specimens were operated with high purity hydrogen in an oil fired furnace (refs. 1 and 5). This showed the need to develop a method to reduce the loss of hydrogen due to permeation.

Testing showed that if an oxide layer was formed on the inside surface of the heater head material, permeability could be reduced by an order of magnitude or more (refs. 1 and 6). This oxide layer can be formed by the addition of an oxygen bearing gas to the hydrogen. Concentrations of 0.5 to 1 percent CO or CO_2 (by volume) were effective (refs. 1, 4, and 6). The overall reaction for forming this oxide is shown below.

$$CO + H_2 + \text{Metal} = \text{Metal Oxide} + H_2O + H_2 + CH_4$$

or

$$CO_2 + H_2 + \text{Metal} = \text{Metal Oxide} + H_2O + H_2 + CH_4$$

It is believed that the water that is formed plays an important role because it too is an oxygen bearing gas. This reaction is shown below.

$$H_2O + \text{Metal} = \text{Metal Oxide} + H_2$$

The oxide that was formed typically had a thickness of 1 to 3 μm, and had calculated permeabilities that are four to five times lower in order of magnitude than the bulk permeability or the material without the inner oxide (refs. 1 and 6). The CO or CO_2 dopant breaks down in the presence of high temperature hydrogen to form water and methane. Figure 3 shows experimental and theoretical results for the breakdown of CO_2 in high temperature hydrogen. The theoretical results were obtained using a kinetics code described in reference 7 and are shown by the solid and dotted lines, with the solid line showing the formation of water and the intermediate formation of CO. The dotted lines show the loss of CO_2 and the formation of CH_4. These theoretical results show that the breakdown of CO_2 is a two step process, the first step being the formation of water and CO. This first step is very fast, being well under way in 17 min. The second step in the breakdown is for the CO to form methane and more water. Theoretical kinetics show that this final step should be very slow, not being complete for several months.

The breakdown of 1 percent CO_2 (by volume) is shown below.

Step 1 $\quad CO_2 + 99\ H_2 = CO + H_2O + 98\ H_2$

Step 2 $\quad CO + H_2O + 98\ H_2 = CH_4 + 2\ H_2O + 95\ H_2$

Overall Reaction

$$CO_2 + 99\ H_2 = CH_4 + 2\ H_2O + 95\ H_2$$

Experimental results from rig and engine tests showed high levels of methane after a very short period of time. These points are shown on figure 3. This methane would not have occurred unless both steps 1 and 2 occur much more rapidly than predicted. This suggests that the water formed is the ultimate oxygen bearing gas inside the engine and that it is rapidly formed.

The typical Stirling engine system shuttles hydrogen between several distinct volumes. Three of the major volumes of interest are:

1. The heater head which will have metal temperatures of 700 to 900 °C, and is where the loss of hydrogen by permeation takes place,

2. The engine cooler and regenerator with the cooler operating at a nominal 50 °C, and

3. The hydrogen storage bottle which normally operates at ambient temperature.

It should be pointed out that the test rig, which is described later, is a static rig that simulates only the heater head region of the engine. It does not provide for any mass flows to and from lower temperature regions that would occur in an actual engine. It is because of this lack of mass flows in the simulator rig that the effect that water can have on hydrogen permeability was not observed until later testing.

Testing at NASA Lewis and at United Stirling in Sweden of a P-40 engine with 1 percent CO_2 (by volume) has shown that water can condense in the engine cooler and regenerator (ref. 2). This condensation of water, coupled with the rapid breakdown of the CO or CO_2 originally in the hydrogen, provides a mechanism to remove most of the oxygen bearing gas from the engine. The content of the oxygen bearing gas will then be determined by the lowest temperature that the hydrogen working fluid is exposed to.

When the content of the oxygen bearing gas is lowered to a low enough level by condensation, the resulting dry hydrogen can chemically reduce the heater tube inner oxide, which again can condense on the low temperature surfaces in the engine system. This process of chemically reducing the oxide and condensing of the water can continue until the heater head of the engine is in an unoxidized, high permeability state.

RESULTS AND DISCUSSION

Tubes which had been previously fully oxidized by long term exposure to hydrogen with 1 percent CO_2 (by volume) were exposed to a variety of hydrogen mixtures for up to 20 cycles of 5 hr each. The mixtures (table I) contained nominally 0, 265, 380, 530, 750, 1,500 ppm CO and 500 ppm CO_2. Permeability was calculated from the rate of pressure decay for each cycle. The data obtained, in terms of permeability versus number of cycle exposure, is shown in figures 4 to 11. The results are summarized in figure 12.

High Purity Hydrogen

Figure 4 shows permeability versus cycles for testing that was done with high purity hydrogen. All three modules showed increases in permeability. Actual permeabilities for material in a totally deoxidized state would be expected to be higher. The highest permeability observed was 3.5×10^{-6} $cm^2/sec\ MPa^{0.5}$.

265 ppm CO

265 ppm CO was used to provide a derived water content of 265 ppm. All modules tested at this concentration showed significant increases in permeability, with the highest that was observed being 2.3×10^{-6} $cm^2/sec\ MPa^{0.5}$. The results for this concentration are shown in figure 5.

380 ppm CO

380 ppm CO was used to provide a water concentration of 380 ppm, with the results shown in figure 6. These modules did not exhibit any deoxidation. This concentration differs from the next higher tested by having a dew point approximately 12 °C lower.

530 ppm CO

530 ppm CO was used to provide a water concentration of 530 ppm. Two of the three modules tested at this water content showed significant deoxidation with the highest observed being 1.7×10^{-6} $cm^2/sec\ MPa^{0.5}$. These results are plotted in figure 7.

750 ppm CO

All permeabilities at this total oxygen level remained stable and low, and are plotted in figure 8.

500 ppm CO_2

500 ppm CO_2 was used to provide a water concentration of 1000 ppm. Two tube sets remained at stable low permeability. One module gave what is believed to be anomalous data. This outlier is not shown in figure 12, which shows permeability as a function of water content. Possible causes include pressure transducer problems or that the module and fittings would leak when hot. It should be safe to disregard this data due to the high permeability during the first 5-hr cycle, which is a cycle during which little change in permeability would be expected. This data is presented in figure 9.

1500 ppm CO and Higher Dopant Concentrations

All data taken at 1500 and 2000 ppm CO showed stable low permeability. Dopant levels above 2000 ppm total oxygen were not used as a part of this study, except for 1 percent CO_2 (by volume) which was used to form the initial oxide layer. Previous work by Misencik has shown that concentrations of 5000 and 10 000 ppm CO are not only effective at maintaining a stable oxide and low permeability, they are also effective at forming the initial low permeability oxide (ref. 5). The data for 1500 and 2000 ppm CO is presented in figures 10 and 11.

Permeability Versus Water Content

Figure 12 combines the results of the preceding eight figures into a plot of permeability as a function of derived or equivalent water content. Data from a previous program (ref. 5) is also included and is consistent with the results of this investigation. It would appear that permeability is not at all affected if the water content (equivalent total oxygen) is greater than about 750 ppm. The inference we draw from this is that the protective oxide on the inner surface of the tubes is not reduced or altered if the water content of

the hydrogen is sufficient to maintain the equilibrium previously discussed. At lower values of water content, permeability is affected. From this we infer that the equilibrium is upset and that the oxide layer is acted upon by the drier hydrogen. Although the exact boundary line between equilibrium and non-equilibrium is not clear, it is evident that the oxide layer is susceptible to alteration if the equivalent water content is below 750 ppm.

Metallography

Optical, and scanning electron micrographs were taken of the tube samples that were operated with high purity, and doped hydrogen (380 and 750 ppm CO) and are shown in figures 13 and 14. Schoun and Misencik's work on oxide films (ref. 6) and this study show that permeability can vary significantly even though the general appearance of the oxide remains unchanged. This suggests that an increase in oxide porosity is the first response of the oxide being operated in hydrogen having low water or total oxygen contents.

The optical micrographs that were taken show definite penetration of the oxide into the base metal. This penetrated oxide could act as a source of oxygen when the material is operated with hydrogen having low water content. On the other hand, the subsurface oxide may be more resistant to reduction. This could cause a permanent reduction in permeability for the CG-27 tubes. The data obtained with high purity hydrogen appears to indicate this sort of phenomenon may be present. The apparently anomalous data at 380 ppm may also be the result of such an effect.

CONCLUDING REMARKS

Testing has shown that 750 ppm or more of water is effective in maintaining stable, low permeability in CG-27. Testing with lower total oxygen contents of 0, 265, 380, and 530 ppm equivalent water indicates that resistance to permeation cannot be reliably maintained at these lower levels. The apparent mechanism causing this is the equilibrium between hydrogen, water (or oxygen bearing gas), metal oxide, and the metal being tipped towards the reduction of the oxide and generation of water. As the oxide is chemically reduced, permeation increases until a new equilibrium is again established. If a mechanism exists for condensing the resulting water, reduction may continue until all the oxide is consumed.

In an automotive Stirling engine, the minimum temperature during operation is such that approximately 1000 ppm of water vapor can be maintained. Any water that condensed when the engine is not running and exposed to cold ambient temperatures would be evaporated during operation and should be effective in maintaining the oxide coating and attendant low permeation. However, a typical engine system contains a hydrogen storage reservoir as part of the control system. Here, water could condense and not return to the engine proper. Figure 15 shows the saturation concentration of water in the engine's working fluid that would be determined by the engine cooler and storage bottle temperature. If the water concentration were to be determined by the engine cooler temperature the water content would range between 1000 and 10 000 ppm. The water concentration, if determined by an ambient temperature storage bottle would generally be below 300 ppm and even below 10 ppm on a cold day. It would

appear necessary to provide heating for the reservoir to assure sufficient water vapor in the engine system under all conditions.

REFERENCES

1. Misencik, J.A.: Evaluation of Dopants in Hydrogen to Reduce Hydrogen Permeation in Candidate Stirling Engine Heater Head Tube Alloys at 760° and 820°C. DOE/NASA/51040-41, NASA TM-82920, 1982.

2. Cairelli, J.E.; and Skog, E.: Experimental Evaluation of Working Gas Containment in the Automotive Stirling Engine. Proceedings of the Twenty-First Automotive Technology Development Contractors' Coordination Meeting, SAE P-138, Society of Automotive Engineers, 1983, pp. 47-54.

3. Misencik, J.A.; and Titran, R.H.: Evaluation of Candidate Stirling Engine Heater Tube Alloys after 3,500 Hours Exposure to High Pressure Doped Hydrogen or Helium. DOE/NASA/51040-56, NASA TM-83782, 1984.

4. Misencik, J.A.: Evaluation of CO_2 and CO Dopants in Hydrogen to Reduce Hydrogen Permeation in the Stirling Engine Heater Head Tube Alloy CG-27. DOE/NASA/51040-50, NASA TM-83535, 1983.

5. Misencik, J.A.: Evaluation of Candidate Stirling Engine Heater Tube Alloys for 1,000 Hours at 760°C. DOE/NASA/1040-18, NASA TM-81578, 1980.

6. Schoun, S.R.; and Misencik, J.A.: Effect of Oxide Films on Hydrogen Permeability of Candidate Stirling Heater Head Tube Alloys. DOE/NASA/51040-38, NASA TM-82824, 1981.

7. Bittker, D.A.; and Scullin, V.J.: GCKP84 - General Chemical Kinetics Code for Gas-Phase, Flow and Batch Processes Including Heat Transfer Effects. NASA TP-2320, 1984.

TABLE I. - COMPOSITION OF HYDROGEN USED IN TESTING

[Concentrations in ppm unless otherwise noted. Percentages are on a volume basis. O_2, CO_2, N_2, CH_4, and CO_2 analysis performed by gas chromatagraphy. H_2O analysis performed with a CO_2 cooled dewpointer.]

Vendor analysis	NASA analysis					
	O_2	CO	N_2	CH_4	CO_2	H_2O
High purity	4		5	<1	<2	NA
High purity	4		3	<1	<2	
265 ppm CO	8	270	601	<2	<2	44
380 ppm CO	9	356	611		<2	
530 ppm CO	9	531	544	<2	<2	51
753 ppm CO	<3	751	509	<2	<2	92
500 ppm CO_2	<3	<10	15	<2	492	<8
1500 ppm CO	<3	1386	21	<2	22	<8
1% CO_2	<20				1.03%	<50

TABLE II. - PRESSURE DECAY DATA AND CALCULATED PERMEABILITY COEFFICIENT FOR SELECTED 5 HOUR CYCLES

(a) Test modules filled with high purity hydrogen

Cycle	Module 1			Module 10			Module 2		
	Start	End	Hydrogen permeability coefficient, φ, $cm^2/sec\ MPa^{0.5}$	Start	End	Hydrogen permeability coefficient, φ, $cm^2/sec\ MPa^{0.5}$	Start	End	Hydrogen permeability coefficient, φ, $cm^2/sec\ MPa^{0.5}$
	Pressure, MPa			Pressure, MPa			Pressure, MPa		
1	11.82	10.44	0.55×10^{-6}	12.61	10.57	0.72×10^{-6}	3.34	2.94	0.30×10^{-6}
5	-----	-----	---------	-----	-----	---------	----	----	---------
10	11.27	7.07	1.85×10^{-6}	12.10	9.27	1.15×10^{-6}	3.19	2.43	$.60 \times 10^{-6}$
15	11.09	5.17	2.81×10^{-6}	12.58	10.37	$.86 \times 10^{-6}$	3.29	1.60	1.47×10^{-6}
20	10.58	5.96	2.47×10^{-6}	11.96	10.41	$.71 \times 10^{-6}$	3.39	1.96	1.32×10^{-6}
25	12.37	4.86	3.48×10^{-6}	12.48	9.55	1.17×10^{-6}	3.13	1.35	1.35×10^{-6}

(b) Test modules filled with 265 ppm CO

Cycle	Module 8			Module 12			Module 1		
	Start	End	Hydrogen permeability coefficient, φ, $cm^2/sec\ MPa^{0.5}$	Start	End	Hydrogen permeability coefficient, φ, $cm^2/sec\ MPa^{0.5}$	Start	End	Hydrogen permeability coefficient, φ, $cm^2/sec\ MPa^{0.5}$
	Pressure, MPa			Pressure, MPa			Pressure, MPa		
1	13.7	12	0.61×10^{-6}	13.3	9.75	1.16×10^{-6}	3.96	3.31	0.45×10^{-6}
5	13.3	11.6	$.6 \times 10^{-6}$	12.2	6.8	1.99×10^{-6}	3.58	2.64	$.71 \times 10^{-6}$
10	13.3	10.6	1×10^{-6}	12.1	6.4	1.15×10^{-6}	3.58	2.64	$.71 \times 10^{-6}$
15	13.5	11	$.97 \times 10^{-6}$	12.6	8.1	1.57×10^{-6}	----	----	---------
20	13.89	11	1.06×10^{-6}	13.3	8.51	1.62×10^{-6}	----	----	---------

(c) Test modules filled with 380 ppm CO

Cycle	Module 7			Module 8			Module 9			Module 11		
	Start	End	Hydrogen permeability coefficient, φ, $cm^2/sec\ MPa^{0.5}$	Start	End	Hydrogen permeability coefficient, φ, $cm^2/sec\ MPa^{0.5}$	Start	End	Hydrogen permeability coefficient, φ, $cm^2/sec\ MPa^{0.5}$	Start	End	Hydrogen permeability coefficient, φ, $cm^2/sec\ MPa^{0.5}$
	Pressure, MPa			Pressure, MPa			Pressure, MPa			Pressure, MPa		
1	13.13	11.58	0.59×10^{-6}	6.82	5.89	0.49×10^{-6}	3.51	3.20	0.22×10^{-6}	3.51	2.72	0.50×10^{-6}
5	-----	-----	---------	----	----	---------	----	----	---------	----	----	---------
10	12.47	11	$.57 \times 10^{-6}$	6	5.24	$.42 \times 10^{-6}$	3.39	2.89	$.37 \times 10^{-6}$	3.19	1.92	$.88 \times 10^{-6}$
15	11.61	9.89	$.58 \times 10^{-6}$	5.78	4.96	$.47 \times 10^{-6}$	3.29	2.82	$.35 \times 10^{-6}$	3.07	2.63	$.28 \times 10^{-6}$
20	11.55	9.86	$.58 \times 10^{-6}$	5.93	5.34	$.38 \times 10^{-6}$	3.43	3.13	$.25 \times 10^{-6}$	3.93	2.82	$.67 \times 10^{-6}$

TABLE II. - Continued.

(d) Test modules filled with 530 ppm CO

Cycle	Module 5			Module 11			Module 2		
	Start	End	Hydrogen permeability coefficient, φ, $cm^2/sec\ MPa^{0.5}$	Start	End	Hydrogen permeability coefficient, φ, $cm^2/sec\ MPa^{0.5}$	Start	End	Hydrogen permeability coefficient, φ, $cm^2/sec\ MPa^{0.5}$
	Pressure, MPa			Pressure, MPa			Pressure, MPa		
1	13.2	11.1	0.79×10^{-6}	13.1	10.2	0.93×10^{-6}	3.67	2.99	0.49×10^{-6}
5	12.8	10.9	$.75 \times 10^{-6}$	12.4	7.8	1.62×10^{-6}	3.44	1.97	1.19×10^{-6}
10	13	10.8	$.83 \times 10^{-6}$	12.7	7.7	1.74×10^{-6}	3.13	1.56	1.38×10^{-6}
15	13.1	11.3	$.68 \times 10^{-6}$	12.4	8.8	1.41×10^{-6}	----	----	---------
20	13.5	11.5	$.78 \times 10^{-6}$	13.3	9	1.44×10^{-6}	----	----	---------

(e) Test modules filled with 750 ppm CO

Cycle	Module 10			Module 5			Module 6			Module 12		
	Start	End	Hydrogen permeability coefficient, φ, $cm^2/sec\ MPa^{0.5}$	Start	End	Hydrogen permeability coefficient, φ, $cm^2/sec\ MPa^{0.5}$	Start	End	Hydrogen permeability coefficient, φ, $cm^2/sec\ MPa^{0.5}$	Start	End	Hydrogen permeability coefficient, φ, $cm^2/sec\ MPa^{0.5}$
	Pressure, MPa			Pressure, MPa			Pressure, MPa			Pressure, MPa		
1	13.96	12.2	0.65×10^{-6}	6.44	5.96	0.26×10^{-6}	3.72	3.49	0.16×10^{-6}	3.76	2.79	0.60×10^{-6}
5	12.96	11.06	$.73 \times 10^{-6}$	----	----	---------	----	----	---------	----	----	---------
10	12.65	10.96	$.65 \times 10^{-6}$	6	5.13	$.48 \times 10^{-6}$	3.44	2.91	$.40 \times 10^{-6}$	3.53	2.10	$.96 \times 10^{-6}$
15	12.65	11.13	$.62 \times 10^{-6}$	6	5.13	$.48 \times 10^{-6}$	3.44	2.91	$.40 \times 10^{-6}$	4.05	2.81	$.86 \times 10^{-6}$
20	12.79	11.17	$.62 \times 10^{-6}$	6.34	5.69	$.41 \times 10^{-6}$	3.73	3.41	$.26 \times 10^{-6}$	3.45	2.38	$.70 \times 10^{-6}$

(f) Test modules filled with 530 ppm CO_2

Cycle	Module 7			Module 6			Module 3		
	Start	End	Hydrogen permeability coefficient, φ, $cm^2/sec\ MPa^{0.5}$	Start	End	Hydrogen permeability coefficient, φ, $cm^2/sec\ MPa^{0.5}$	Start	End	Hydrogen permeability coefficient, φ, $cm^2/sec\ MPa^{0.5}$
	Pressure, MPa			Pressure, MPa			Pressure, MPa		
1	13.5	12.2	0.50×10^{-6}	13.5	12.4	0.40×10^{-6}	3.66	1.48	1.85×10^{-6}
5	13.4	12.2	$.46 \times 10^{-6}$	13.4	12.6	$.30 \times 10^{-6}$	3.50	1.47	1.75×10^{-6}
10	13.7	12.1	$.61 \times 10^{-6}$	10.9	10.2	$.28 \times 10^{-6}$	3	1.34	1.51×10^{-6}
15	----	----	---------	13.8	12.5	$.39 \times 10^{-6}$	----	----	---------

TABLE II. - Concluded.

(g) Test modules filled with 1500 ppm CO

Cycle	Module 7			Module 8			Module 9			Module 11		
	Start	End	Hydrogen permeability coefficient, φ, $cm^2/sec\ MPa^{0.5}$	Start	End	Hydrogen permeability coefficient, φ, $cm^2/sec\ MPa^{0.5}$	Start	End	Hydrogen permeability coefficient, φ, $cm^2/sec\ MPa^{0.5}$	Start	End	Hydrogen permeability coefficient, φ, $cm^2/sec\ MPa^{0.5}$
	Pressure, MPa			Pressure, MPa			Pressure, MPa			Pressure, MPa		
1	13.61	12.24	0.51×10^{-6}	6.51	6.06	0.24×10^{-6}	3.54	3.03	0.37×10^{-6}	3.69	3.13	0.33×10^{-6}
5	13.06	11.58	$.56 \times 10^{-6}$	6.39	5.69	$.38 \times 10^{-6}$	3.58	3.23	$.24 \times 10^{-6}$	3.43	3	$.27 \times 10^{-6}$
10	13.34	11.68	$.62 \times 10^{-6}$	6.29	5.58	$.38 \times 10^{-6}$	3.47	3.19	$.21 \times 10^{-6}$	3.41	2.82	$.37 \times 10^{-6}$
15	13.17	11.68	$.56 \times 10^{-6}$	6.31	5.60	$.38 \times 10^{-6}$	3.35	3.07	$.21 \times 10^{-6}$	----	----	----------
20	13.2	11.68	$.57 \times 10^{-6}$	6.72	6.07	$.34 \times 10^{-6}$	3.72	3.42	$.21 \times 10^{-6}$	----	----	----------

(h) Test modules filled with 2000 ppm CO

Cycle	Module 5			Module 6			Module 12		
	Start	End	Hydrogen permeability coefficient, φ, $cm^2/sec\ MPa^{0.5}$	Start	End	Hydrogen permeability coefficient, φ, $cm^2/sec\ MPa^{0.5}$	Start	End	Hydrogen permeability coefficient, φ, $cm^2/sec\ MPa^{0.5}$
	Pressure, MPa			Pressure, MPa			Pressure, MPa		
1	6.44	6.1	0.18×10^{-6}	3.55	3.41	0.1×10^{-6}	3.44	2.96	0.30×10^{-6}
5	6.12	5.9	$.08 \times 10^{-6}$	3.60	3.44	$.11 \times 10^{-6}$	3.51	2.91	$.38 \times 10^{-6}$
10	6.37	5.96	$.22 \times 10^{-6}$	3.65	3.41	$.17 \times 10^{-6}$	3.38	2.84	$.34 \times 10^{-6}$
15	6.13	5.6	$.29 \times 10^{-6}$	3.38	3.17	$.15 \times 10^{-6}$	----	----	----------
20	6.27	5.77	$.27 \times 10^{-6}$	3.89	3.68	$.14 \times 10^{-6}$	----	----	----------

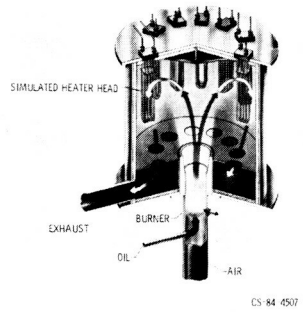

FIGURE 1. - SCHEMATIC OF TEST RIG.

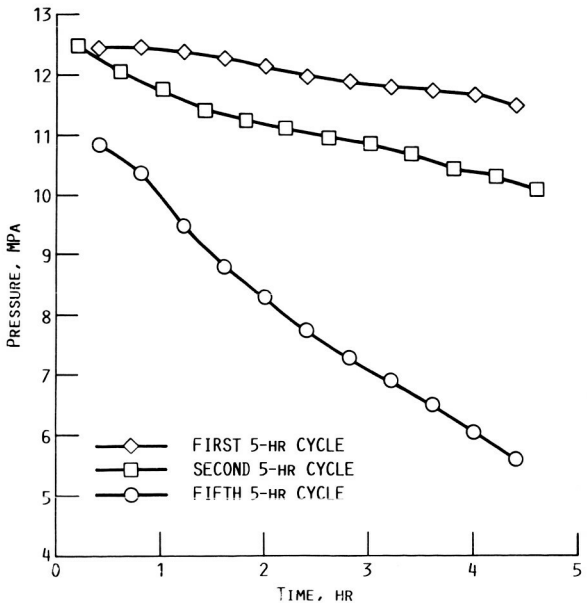

FIGURE 2. - TYPICAL PRESSURE DECAY CURVES FOR CG-27, NEW TUBES, 1% CO_2 BALANCE H_2, TEMPERATURE 820 ^{o}C.

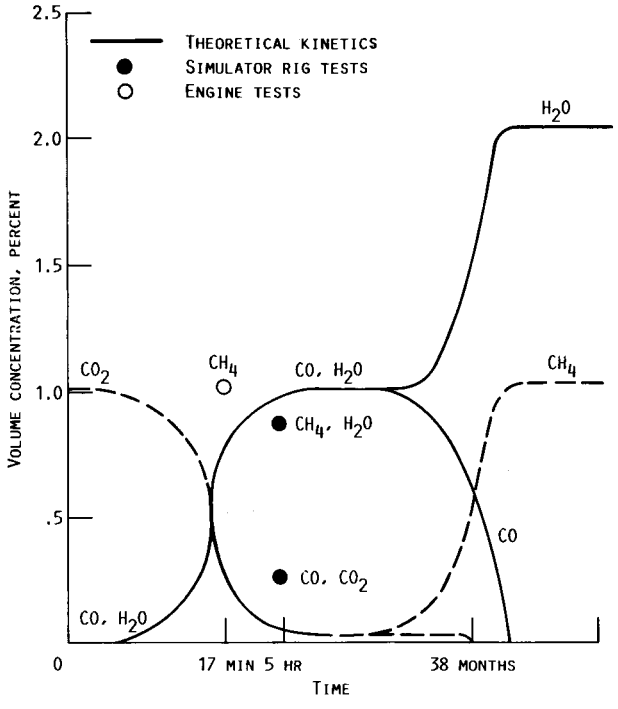

FIGURE 3. - DOPED HYDROGEN KINETICS: PRESSURE 10.5 MPA; TEMPERATURE 730 ^{o}C; 1% CO_2 BY VOLUME BALANCE H_2.

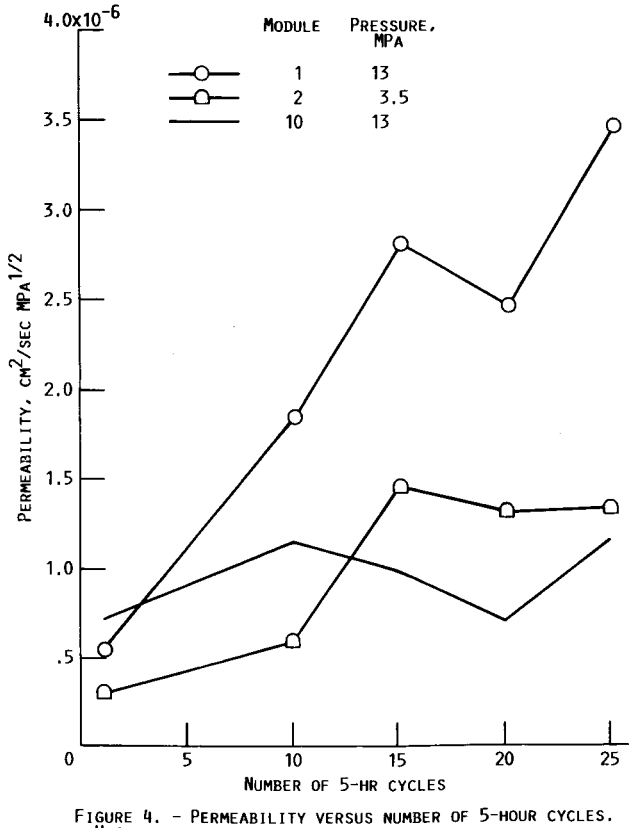

FIGURE 4. - PERMEABILITY VERSUS NUMBER OF 5-HOUR CYCLES. HIGH PURITY HYDROGEN.

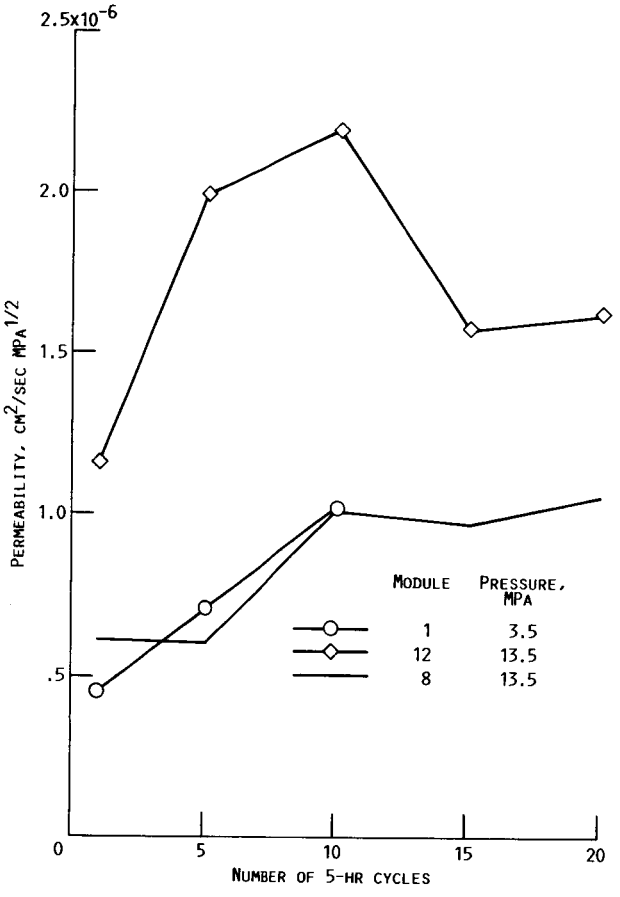

FIGURE 5. - PERMEABILITY VERSUS NUMBER OF 5-HOUR CYCLES. 265 PPM H_2O (DERIVED FROM 265 PPM CO) BALANCE H_2.

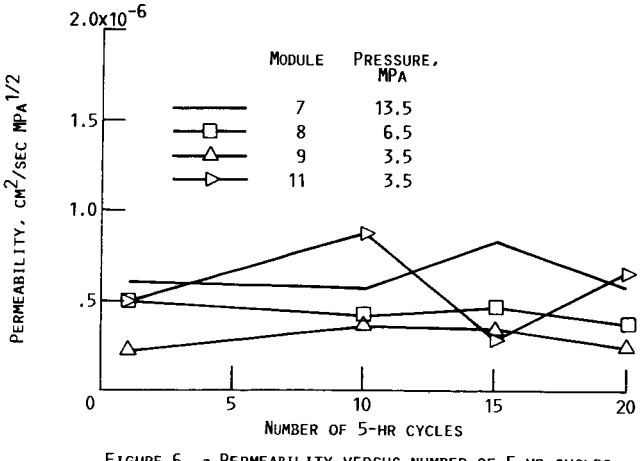

FIGURE 6. - PERMEABILITY VERSUS NUMBER OF 5-HR CYCLES. 380 PPM H_2O (DERIVED FROM 380 PPM CO) BALANCE H_2.

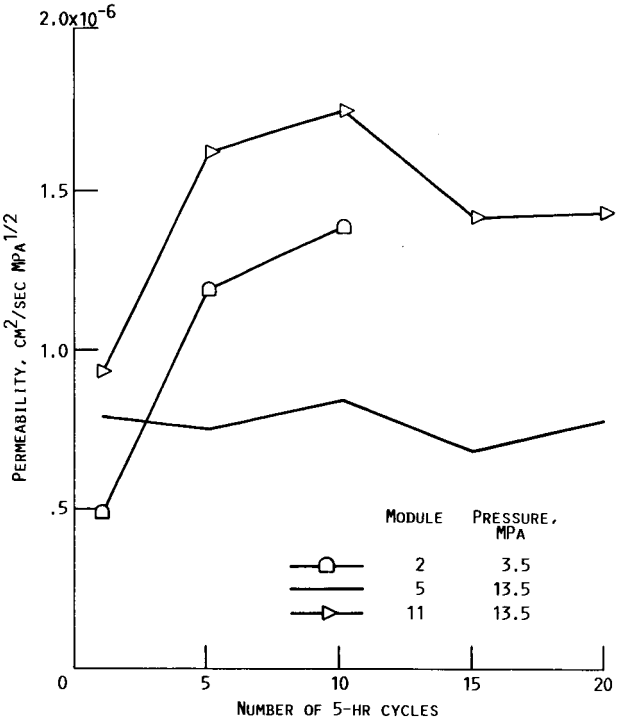

FIGURE 7. - PERMEABILITY VERSUS NUMBER OF 5-HOUR CYCLES. 530 PPM H_2O (DERIVED FROM 530 PPM CO) BALANCE H_2.

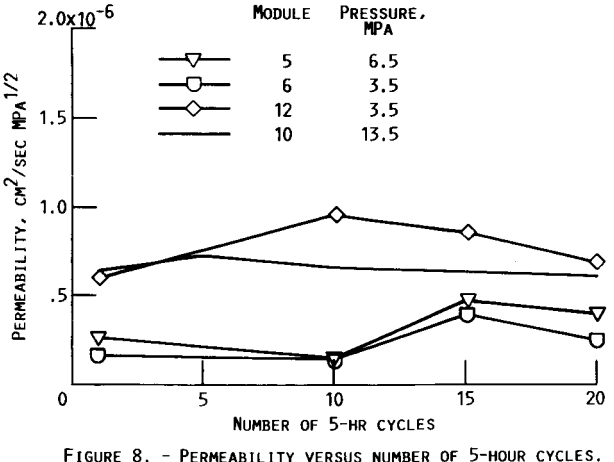

FIGURE 8. - PERMEABILITY VERSUS NUMBER OF 5-HOUR CYCLES. 750 PPM H_2O (DERIVED FROM 750 PPM CO) BALANCE H_2.

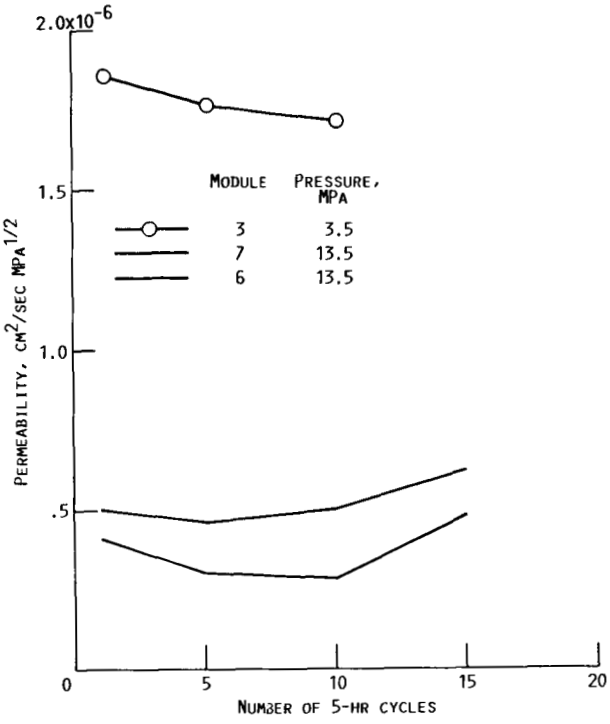

FIGURE 9. - PERMEABILITY VERSUS NUMBER OF 5-HOUR CYCLES. 1000 PPM H_2O (DERIVED FROM 500 PPM CO_2) BALANCE H_2.

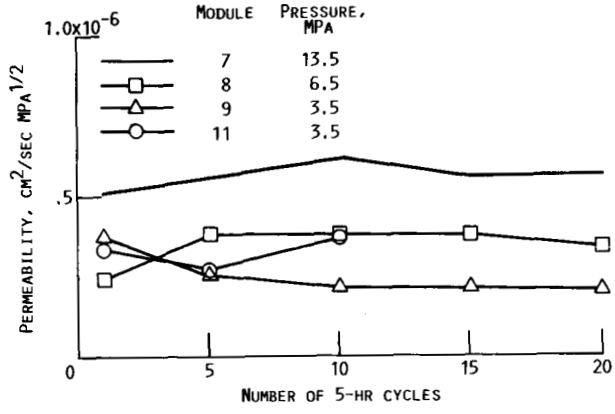

FIGURE 10. - PERMEABILITY VERSUS NUMBER OF 5-HOUR CYCLES. 1500 PPM H_2O (DERIVED FROM 1500 PPM CO) BALANCE H_2.

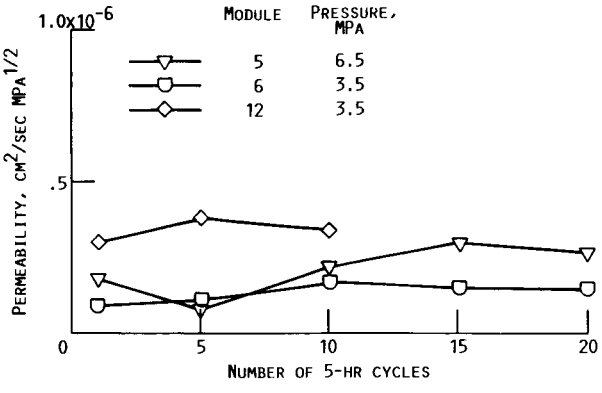

Figure 11. - Permeability versus number of 5-hour cycles. 2000 ppm H_2O (derived from 2000 ppm CO) balance H_2.

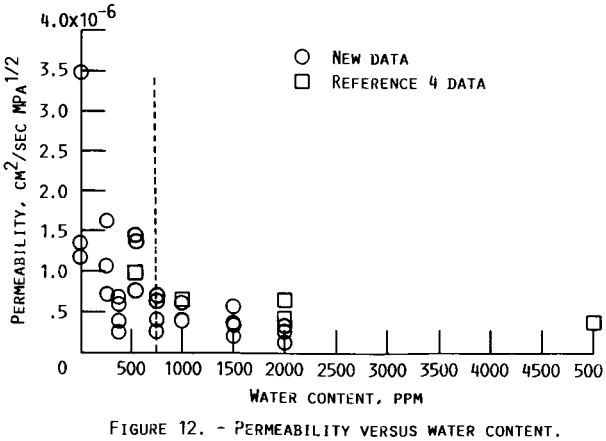

Figure 12. - Permeability versus water content.

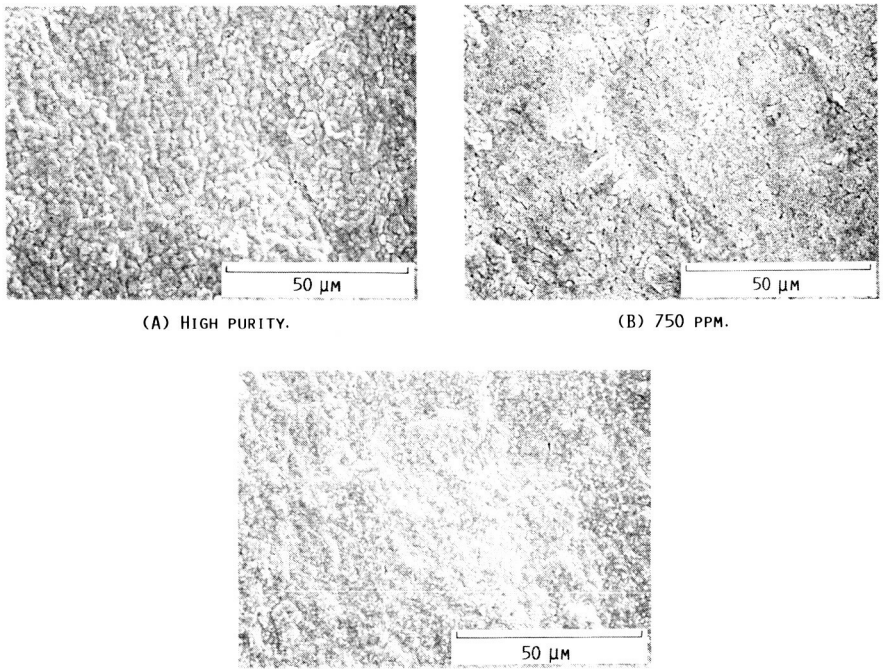

(A) HIGH PURITY.

(B) 750 PPM.

(C) 380 PPM.

FIGURE 13. - SCANNING ELECTRON MICROGRAPHS OF INNER SURFACE OF CG-27.

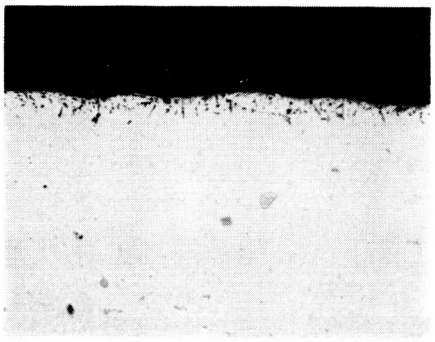

(A) HIGH PURITY.

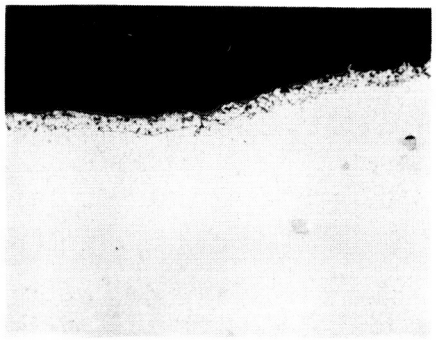

(B) 750 PPM.

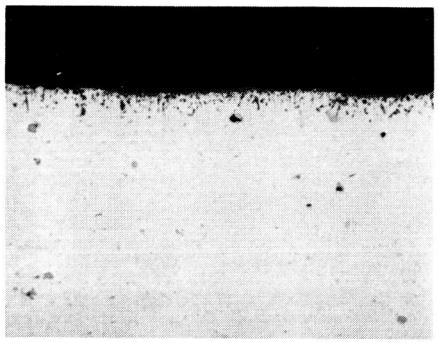

(C) 380 PPM CO.

FIGURE 14. - UNETCHED OPTICAL CROSSECTIONS OF INSIDE SURFACE OF CG-27.

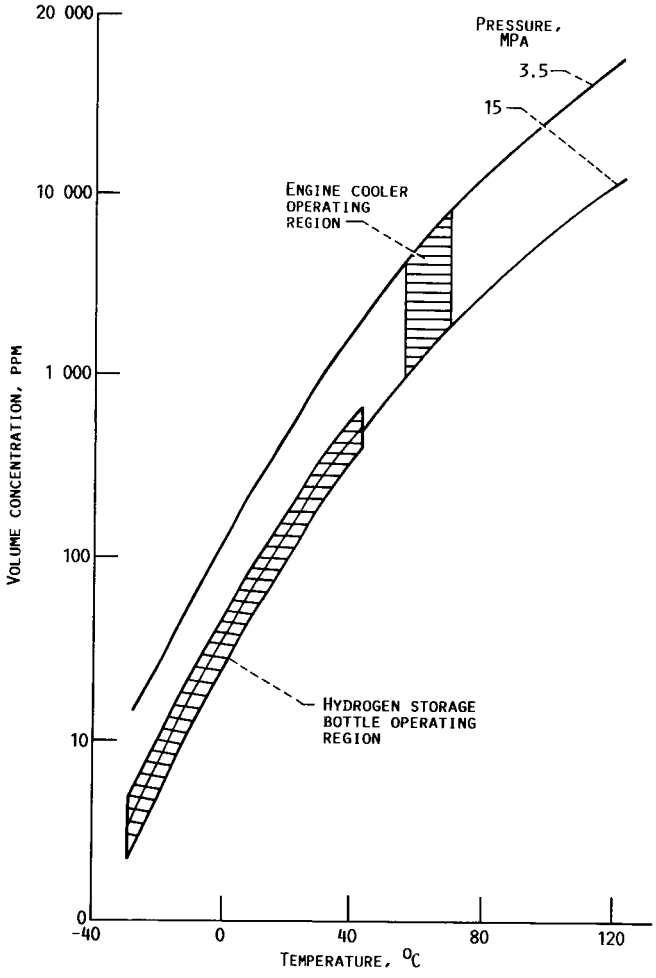

FIGURE 15. - SATURATION CONCENTRATION OF WATER.

1. Report No.	2. Government Accession No.	3. Recipient's Catalog No.
NASA TM-88898		

4. Title and Subtitle	5. Report Date
Effect of Water on Hydrogen Permeability	January 1987
	6. Performing Organization Code 778-35-13
7. Author(s) David Hulligan and William A. Tomazic	8. Performing Organization Report No. E-3321
	10. Work Unit No.
9. Performing Organization Name and Address Sverdrup Technology, Inc., Middleburg Heights, Ohio, and National Aeronautics and Space Administration, Lewis Research Center, Cleveland, Ohio 44135	11. Contract or Grant No.
	13. Type of Report and Period Covered Technical Memorandum
12. Sponsoring Agency Name and Address U.S. Department of Energy Office of Vehicle and Engine R&D Washington, D.C. 20545	14. Sponsoring Agency ~~Code~~ Report No. DOE/NASA/50112-68

15. Supplementary Notes

Final Report. Prepared under Interagency Agreement DE-AI01-85CE50112. David Hulligan, Sverdrup Technology, Inc., Middleburg Heights, Ohio, and William A. Tomazic, NASA Lewis Research Center, Cleveland, Ohio 44135.

16. Abstract

Doping of hydrogen with CO and CO_2 was developed to reduce hydrogen permeation in Stirling engines by forming a low permeability oxide coating on the inner surface of the heater head tubes. Although doping worked well, under certain circumstances the protective oxide could be chemically reduced by the hydrogen in the engine. Some oxygen is required in the hydrogen to prevent reduction. Eventually, all the oxygen in the hydrogen gas - whatever its source - shows up as water. This is the result of hydrogen reducing the CO, CO_2, or the protective inner surface oxides. This water can condense in the engine system under the right conditions. If the concentration of water vapor is reduced to a low enough level, the hydrogen can chemically reduce the oxide coating, resulting in an increase in permeability. This work was done to define the minimum water content required to avoid this reduction in the oxide coating. The results of this testing show that a minimum of approximately 750 ppm water is required to prevent an increase in permeability of CG-27, a high temperature metal alloy selected for Stirling engine heater tubes.

17. Key Words (Suggested by Author(s))	18. Distribution Statement
Stirling engine; Hydrogen; Permeability	Unclassified - unlimited STAR Category 85 DOE Category UC-96

19. Security Classif. (of this report)	20. Security Classif. (of this page)	21. No. of pages	22. Price*
Unclassified	Unclassified		A02

*For sale by the National Technical Information Service, Springfield, Virginia 22161